Photoinduced Intramolecular Charge Transfer Reaction in (*E*)-3-(4-Methylamino-phenyl)-acrylic Acid Methyl Ester: A Fluorescence Study in Combination with TDDFT Calculation

Amrita Chakraborty,[†] Samiran Kar,[†,‡] D. N. Nath,[§] and Nikhil Guchhait[†,*]

Department of Chemistry, University of Calcutta, 92, A.P.C. Road, Kolkata 700009, India, and Department of Physical Chemistry, Indian Association for the Cultivation of Science, Jadavpur, Kolkata 700 032, India

Received: May 16, 2006; In Final Form: September 5, 2006

A donor−acceptor substituted aromatic system (*E*)-3-(4-Methylamino-phenyl)-acrylic acid methyl ester (MAPAME) has been synthesized, and its photophysical behavior obtained spectroscopically has been compared with the theoretical results. The observed dual fluorescence from MAPAME has been assigned to emission from locally excited and twisted intramolecular charge transfer states. The donor and acceptor angular dependency on the ground and excited states potential energy surfaces have been calculated both in vacuo and in acetonitrile solvent using time dependent density functional theory (TDDFT) and TDDFT polarized continuum model (TDDFT-PCM), respectively. Calculation predicts that a stabilized twisted excited state is responsible for red shifted charge transfer emission.

1. Introduction

In recent years photophysical studies on organic molecules having both the electron donor and acceptor groups gained special attention due to their wide applications as electrooptical switches, chemical sensors, and fluorescence probes.[1−4] The molecule 4-(dimethylamino)-benzonitrile (DMABN), a model donor−acceptor substituted aromatic system, shows dual fluorescence in polar solvents. Apart from a 'normal' emission of DMABN originated from the locally excited state in nonpolar solvent, a second 'anomalous' strongly solvent dependent red shifted band is observed in polar solvents. The red shifted band attributed to an intramolecular charge transfer (CT) state generated upon photoexcitation is of basic importance in photosynthesis and plays a dominant role in many photochemical reactions.[5] Hence, various research groups performed experiments on DMABN and related molecules, and theoretical modeling has been given for this phenomena. To rationalize this dual fluorescence phenomenon of DMABN quite a few models have been proposed: twisted intramolecular charge transfer (TICT),[6] wagging intramolecular charge transfer (WICT),[7] rehybridization by intramolecular charge transfer (RICT),[8,9] planar intramolecular charge transfer (PICT),[10] etc. Among them, TICT model has been accepted widely for explaining dual fluorescence in different donor−acceptor systems.[6,11−13] The proposed idea of TICT model is that the initially excited state yields another minimum on the potential energy surface by twisting of donor group, which leads to a decoupling of donor from the acceptor thereby promoting the charge transfer process.

Most of the molecules so far investigated for this type of study mainly have tertiary amino group as charge donor. There are only two examples where secondary amine was used as donor in some ortho substituted aromatic system,[14,15] and the idea behind this type of compound is that the ortho substitution forced the monomethyl amino group to be out of plane of the benzene ring and the pretwisting of secondary amino donor accelerates the CT emission.[11] In our very recent studies[16,17] we have already shown that the secondary aromatic amine without any ortho substitution can also act as a good charge donor. In the present work, we present the photophysical properties of a donor−acceptor substituted aromatic system, namely (*E*)-3-(4-methylamino-phenyl)-acrylic acid methyl ester (MAPAME) (Scheme 1), where the same secondary amino group, −NHMe is used as charge donor and −COOMe group as acceptor. Structurally both the donor and acceptor groups are planar to the benzene ring and are different from the other studied system where donor and acceptor groups are pretwisted in the ground state.[16,17] The presence of a double bond between the benzene ring and the acceptor group imparts an extra flexibility to the system. Now in the TICT model, the ICT state should be associated with the diffusive rotational motion of either the donor group, i.e., monomethylamino group or the acceptor, i.e., methylacrylate group attached with benzene moiety. We have used TDDFT method[18−21] as a tool to evaluate the excited state phenomenon in the light of TICT mechanism. Spectroscopy of MAPAME suggested different kinds of behaviors in different kind of solvents, and emission characteristics of the locally excited (LE) and the TICT states solely depend on solvent properties. As the spectral features and dynamical processes strongly depend on solvation, consideration of solute−solvent interaction is important to obtain an accurate under-

SCHEME 1: (*E*)-3-(4-Methylamino-phenyl)-acrylic Acid Methyl Ester

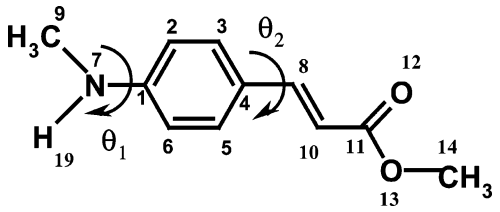

* Corresponding author. E-mail: nguchhait@yahoo.com.
† University of Calcutta.
‡ Present address: CHEMGEN Pharma International, Dr. Siemens Street, Bolck GP, Sect. V, Salt Lake City, Kolkata 700 091, India.
§ Indian Association for the Cultivation of Science.

10.1021/jp0629846 CCC: $33.50
Published on Web 10/18/2006

standing of the experimental observations. Therefore, we have extended our calculation to solvated system using polarized continuum model (PCM), as TDDFT-PCM calculations can provide a good agreement between observed and calculated excitation and emission energies.[22]

2. Methods

p-Nitro benzaldehyde and methyl (triphenyl phosphanylidene) acetate ($Ph_3P{=}CH{-}COOMe$) in dry dichloromethane were stirred at room temperature for 24 h. Generated nitro product was reduced by using zinc and saturated aqueous ammonium chloride solution in methanol at 50 °C to produce methyl-3-(4-amino-phenyl)-acrylate. Then one hydrogen atom of amino group was blocked by di-*tert*- butyl pyrocarbonate (BOC-anhydride) in the presence of triethylamine in THF to produce methyl-3(4-[*N*-(*tert*-butoxycarbonyl)-amino]-phenyl)-acrylate. In the next step, the hydrogen atom of BOC protected amino group was replaced by methyl group by using methyl iodide in the presence of sodium hydride base in DMF solvent at 0 °C. Now BOC group was removed by using trifluroaccetic acid in dichloromethane to produce (*E*)-3-(4-methylamino-phenyl)-acrylic acid methyl ester. The final product was purified by column chromatography and repeated crystallization. ^{1}HNMR (300 MHz, $CDCl_3$) δ 2.87 (s, 3H), 3.77 (s, 3H), 6.18 (d, J = 15.87 Hz, 1H), 6.55 (d, J = 8.67 Hz, 2H), 7.36 (d, J = 8.61 Hz, 2H), 7.58 (d, J = 15.87 Hz, 1H). FTIR (ν_{cm}^{-1}) 819, 987, 1174, 1311, 1572, 1614, 1703, 2927, 3404.

The absorption and emission spectra of MAPAME were recorded on a Hitachi UV/Vis (U-3501) spectrophotometer and Perkin-Elmer (LS50B) fluorimeter, respectively. All the spectral measurements were done at $\sim 10^{-6}$ M concentration of solute in order to avoid aggregation and self-quenching. Solvents used for all measurements were of spectral grade from Spectrochem. The quantum yields were measured by secondary standard method using β-naphthol in cyclohexane (ϕ_f = 0.23) as secondary standard.[23]

Time Master fluorimeter from Photon Technology International (PTI) was used to measure fluorescence lifetime.[24] A thyratron gated nitrogen flash lamp (width ~ 1.5 ns) of 337 nm light is used to excite the sample. The system measures fluorescence lifetime at a flash rate of 25 kHz using PTIs patented strobe technique and gated detection method. Lamp function was measured at the excitation wavelength of 337 nm using Ludox as the scatterer using slits of band-pass of 3 nm. Intensity decay curves were fitted as a sum of exponential terms: where α_i is a preexponential factor representing the fractional

$$F(t) = \sum_i \alpha_i \exp(-t/\tau_i)$$

contribution to the time resolved decay of the component with a lifetime τ_i. The software FeliX32 is used for data acquisition and analysis. The decay parameters were recovered using a nonlinear least squares iterative fitting procedure based on Marguardt algorithms.[25]

The calculations of the structure and the potential energy surfaces have been performed using Gaussian 03 package.[26] The geometry optimization was done by density functional theory (DFT) with hybrid functional B3LYP and 6-311++G(d,p) basis set. Different starting geometries have been used for optimization to obtain the global minimum structure. The analysis of excited state properties has been done by time dependent density functional theory (TDDFT) using the same functional and basis set.[19] In the case of several reported donor−acceptor charge transfer problems, TDDFT is found to be an attractive method due to its computation cost and precision, and it also shows the same quality results as multi-reference double-excitation configuration interaction (MRD-CI) method.[27] The excited state can be modeled in the presence of solvents using the same TDDFT method including polarized continuum model (PCM).[28,29] However, it is seen that TDDFT with approximate functionals encounters problems in the case of dissociating molecules.[30] Also, excitations involving a large change in the charge density tend to be underestimated by TDDFT method as exchange−correlation functionals are too local.[31] Recently Nuegebauer et al. showed the failure of TDDFT to describe long-range CT excitations for calculating electronic transition energy when the large system was composed of several weakly interacting units.[32] However, there are various examples where TDDFT has been used successfully to evaluate the excited state properties.[16−21,33−35] In our calculation using TDDFT method the computed transition energies are the single point energy at the optimized ground state without zero point correction. Calculations of potential energy surfaces have been pursued along the twist coordinate separately at the donor and acceptor sites. We have rotated dihedral angle θ_1 or θ_2 (shown in Scheme 1) for the twisting of the donor group (−NHMe) or the acceptor (− = −COOMe) group. We also extended our calculations in the solvated system using nonequilibrium PCM model. One limitation of our study is that the potential energy surface is computed only along the twisting angle without geometry optimization for various excited states. The validity of such an approach that uses the ground state optimized geometry as a basis of representation of the excited structure has been already successfully established in many recent scientific publications.[18−21,33−35] The difference in energy between the S_0 and S_1 or S_2 states of the calculated PESs without optimization of the excited states at the twisted geometry is considered to be the emission energy.[21] This emission energy value is just an estimation of emission energy and not a theoretical estimate for vertical emission from the excited state since the excited state optimization has not been considered. However, the CIS calculation is used to optimize excited state and to estimate theoretical emission energy.

3. Results and Discussion

The absorption spectra of MAPAME (10^{-6} M) in nonpolar, polar, and hydrogen bonding solvents are shown in Figure 1a. It can be seen from the spectra that the molecule shows two absorption bands at ~318 nm and ~350 nm. These two bands are assigned to the transition from S_0 to S_2 and S_1 states, respectively, as was assigned for other studied systems.[16,17,36] High absorption intensity of the low energy band indicates that this is a $\pi-\pi^*$ type of transition. It is found that the position of the higher energy absorption band is independent of solvent polarity, whereas the position of the lower energy absorption band depends on the polarity of the medium. A slight blue shift of the lower energy absorption band in water may be due to the possible intermolecular hydrogen bonding interaction between the solute molecule and water.

The emission spectra of MAPAME measured in different solvents are shown in Figure 1b, and the spectral data are presented in Table 1. In nonpolar solvent, on 330 nm excitation, MAPAME shows an emission band at ~382 nm, which is nothing but the emission from the locally excited state. But for the same excitation in polar solvents, MAPAME shows dual fluorescence, a short wavelength emission band at ~380 nm, and a long wavelength emission band at ~420−470 nm region. The position of the short wavelength emission band slightly depends on the polarity of the solvent but the long wavelength

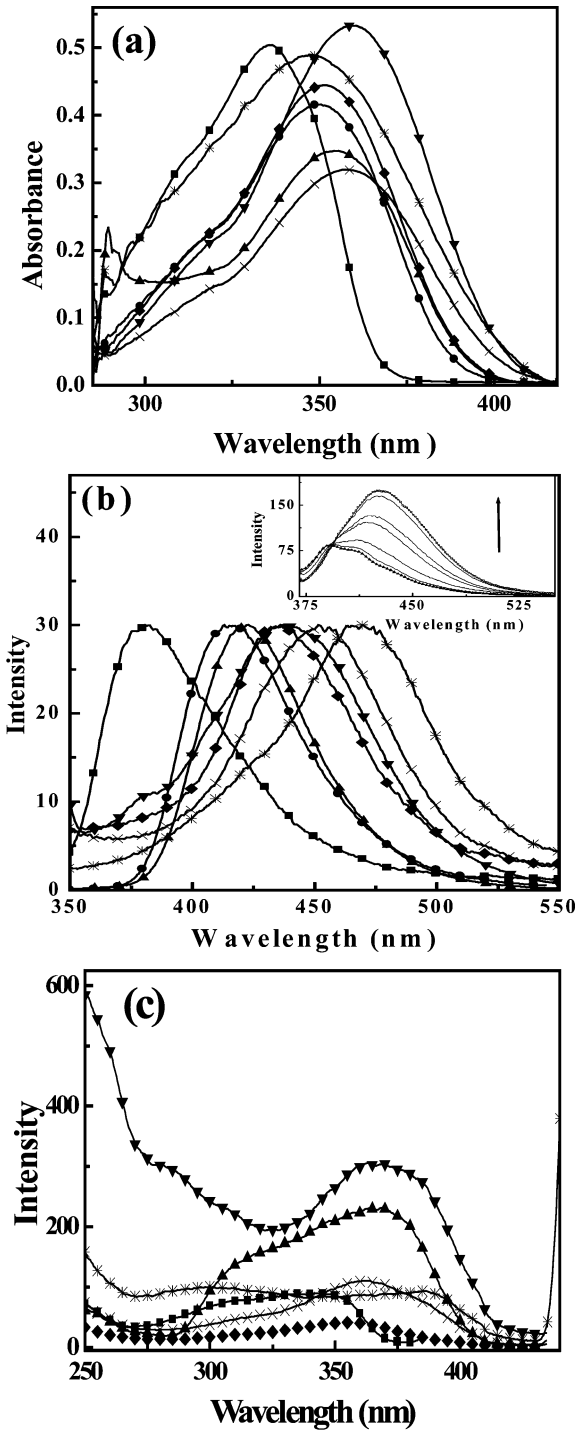

Figure 1. (a) Absorption, (b) emission (λ_{ext} = 330 nm), and (c) excitation spectra of MAPAME in (- ■ -) hexane, (- ● -) dioxane, (- ▲ -) tetrahydrofuran (THF), (- ▼ -) ethanol (- ◆ -), acetonitrile, (- × -) methanol, and (- ∗ -) water. Inset: emission spectra in methylcyclohexane ethanol binary solvent mixture (λ_{ext} = 330 nm, arrow indicates increase of ethanol concentration).

band exhibits solvatochromic red shift with increasing solvent polarity. Comparing this emission band with other similar studied systems the red shifted band is assigned to the emission from the CT state.[11,16,17,36−38] As seen in Figure 1c, the excitation spectra of MAPAME shows bands at ∼318 nm and ∼350 nm, and these bands are indeed similar to that of the absorption spectra. This indicates that the molecule exists as single species in the ground state. The emission in binary solvent mixture (methylcyclohexane + ethanol) is shown in Figure 1b (inset). It is found that the increase of solvent polarity by adding ethanol to methylcyclohexane the charge transfer band becomes more prominent with concomitant decrease in intensity of LE band. The presence of a clear isoemissive point at 392 nm supports that the CT state is generated from LE state.

TABLE 1: Absorption and Emission Bands of MAPAME Molecule in Different Solvents

solvent	λ_{abs} (nm)	λ_{flu} (nm)	Stoke shift, $\Delta\nu_{ST}$ (cm^{-1})
hexane	335, 318	382	3672
carbon tetrachloride	342, 318	394	3859
dioxane	350, 318	414	4417
chloroform	349, 318	420	4844
tetrahydrofuran	353, 318	424	4744
acetonitrile	351, 318	382, 435	5502
ethanol	356, 318	382, 440	5363
methanol	358, 318	382, 453	5858
water	346, 318	382, 470	7626

The solvatochromic measurements in polar aprotic solvent using the Lippert−Mataga equation[39] provide dipole−dipole interactions between the solute and solvents.[40] The following equation (Lippert−Mataga equation) is used for this purpose to calculate the dipole moment of the CT state.

$$\nu_a - \nu_f = \left[\frac{2}{hca^3}\right]\Delta f[\mu^* - \mu]^2$$

$$\Delta f = \left[\frac{\epsilon - 1}{2\epsilon + 1}\right] - \left[\frac{n^2 - 1}{2n^2 + 1}\right]$$

In the above equation h, c, a, μ, and μ^* are Planck's constant, velocity of light, radius of the cavity in which the fluorophore resides, and ground and excited CT state dipole moments, respectively. The term Δf is known as the solvent polarity parameter, and ϵ and n are the dielectric constant and refractive index, respectively, of the medium. The linear dependency of Stokes shift ($\Delta\nu_{ST} = \nu_a - \nu_f$) values of MAPAME in aprotic solvent on solvent parameter Δf is shown in Figure 2a. From the slope of this plot we have calculated the dipole moment of the CT state. The ground state dipole moment (μ) and 'a' values were calculated using hybrid functional B3LYP and 6-311++G(d,p) basis set for the ground state minimum energy structure. The calculated dipole moment for the ground state obtained from DFT calculation and that of the CT state from solvatochromic measurements are 5.46 and 10.0 D, respectively. The high dipole of the CT state indicates that the polarity dependent Stokes shifted emission is arising from different extents of stabilization of the photogenerated charged species in the excited state.

In polar protic solvents a different photophysical phenomenon was observed. The nonlinearity of the Lippert plot indicates a specific solvent−solute interaction, and that may be the hydrogen bonding interaction between MAPAME and the protic solvents. In this case a linear dependency is found between the fluorescence maximum of the red shifted band and the hydrogen bonding parameter (α).[41] This predicts that intermolecular hydrogen bonding can act as an important factor in the ICT path as was observed for some other studied systems.[42] The measured fluorescence quantum yields of MAPAME in different solvents reflect the effect of hydrogen bonding on the ICT process. The measured fluorescence quantum yields at room temperature are presented in Table 2. It is seen that in protic solvent the quantum yields of the CT band markedly decrease with increasing hydrogen bonding parameter α. This indicates the existence of a nonradiative channel of increasing importance with growing hydrogen bonding ability of the solvents results

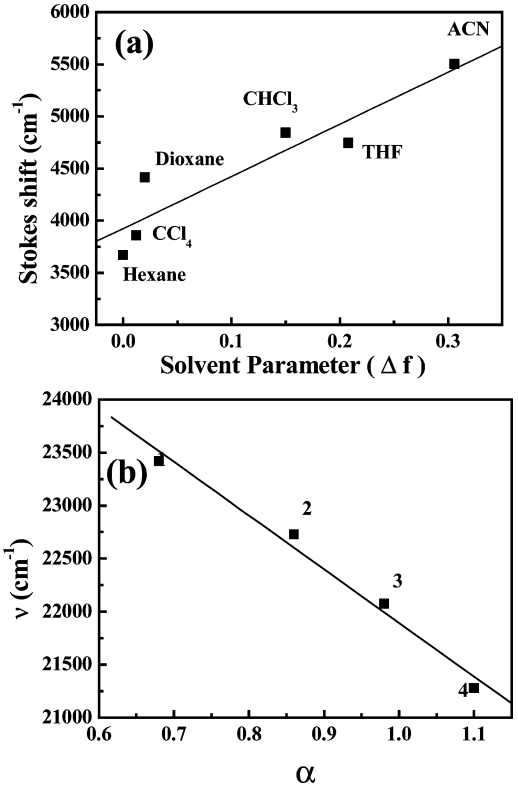

Figure 2. (a) Plot of Stokes shift vs solvent parameter (Lippert plot) and (b) plot of hydrogen bonding parameter (α) vs florescence band position of MAPAME.

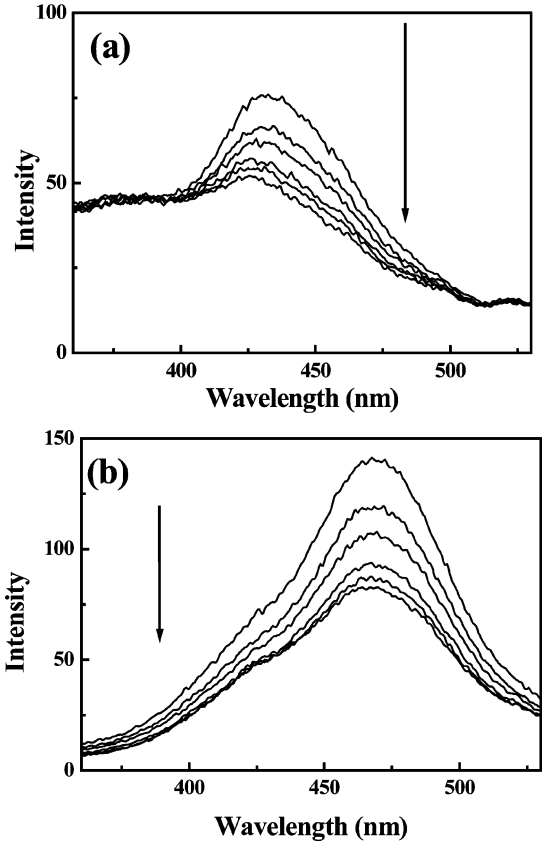

Figure 3. Temperature dependent fluorescence emission spectra of MAPAME in (a) acetonitrile (ACN) (λ_{ext} = 330 nm) and (b) water (λ_{ext} = 330 nm) solvent (arrow indicates increase of temperature from 283 to 333 K with 10 K increment).

in very low fluorescence quantum yields in water. Temperature dependent emission spectra also provide additional support for the presence of a hydrogen bond in protic solvent. As can be seen in Figure 3a, only the intensity of CT emission decreases with increasing temperature in acetonitrile solvent without any change in local emission. The decrease of intensity of the CT band may be due to opening up some temperature activated nonradiative channel. On the other hand, the intensity of both the LE and CT bands in water decreases with increasing temperature (Figure 3b). This may indicate the breaking of the intermolecular hydrogen band of the solvated cluster with increasing temperature, and thereby fluorescence intensity decreases for both bands.

Fluorescence lifetimes in different solvents are presented in Table 2. The fluorescence decay of LE emission of MAPAME in methylcyclohexane is monoexponential with a decay time of ~380 ps and in acetonitrile for the CT band is 400 ps. In acetonitrile solvent, the fluorescence decay of the high energy band is very fast and is beyond the resolution limit of the instrument. In methanol solvent the fluorescence decay time of the 450 nm band is 280 ps. This supports the existence of a nonradiative path due to the hydrogen bonding between the solute and protic solvent.

The fluorescence maximum of MAPAME in methylcyclohexane at 77 K is largely red shifted (~26 nm) (Figure 4) compared to its room temperature spectrum. This spectroscopic change may be due to the aggregates or microcrystallites similar to those reported for aggregates of *trans*-stilbene.[40,43,44] The blue shift of band maximum in ethanol glass matrix with respect to room temperature may be due to the change of solvent properties (polarity, polarizibility, viscosity) upon decrease of temperature or may be due to high viscosity of glass matrix, which may inhibit the geometrical relaxation in the CT state.[40]

The drastic change of absorption and emission spectra of MAPAME in the presence of acid further confirms our assignment about the possible charge transfer process. On addition of 2 N H_2SO_4, a new absorption band appears at ~297 nm which emits at ~365 nm (figure not shown). These absorption and emission bands are typically arising from the $\pi-\pi^*$ transition of chromophore benzene having a conjugated double bond. If acid tries to hydrolyze the ester to form acid, the nature of the absorption and emission bands should not change. Therefore, we can say that the proton binds to the lone

TABLE 2: Quantum Yields and Lifetime of the LE and CT States of MAPAME Molecule in Different Solvents at Room Temperature[a]

solvent	α[a]	quantum yields		lifetime (τ)[b] (ps)	χ^2
		LE state	CT state		
methylcyclohexane	–	1.7×10^{-2}	–	380 (380 nm)	1.14
acetonitrile	–	4.6×10^{-3}	3.3×10^{-2}	400 (435 nm)	1.14
ethanol	0.86	1.4×10^{-3}	2.4×10^{-2}	–	
methanol	0.98	1.5×10^{-3}	1.2×10^{-2}	280 (450 nm)	1.5
water	1.10	1.0×10^{-3}	5.6×10^{-3}	–	

[a] α is the index of solvent hydrogen bond donor ability. [b] Excitation wavelength 337 nm. Values in parentheses indicate the emission monitoring wavelength.

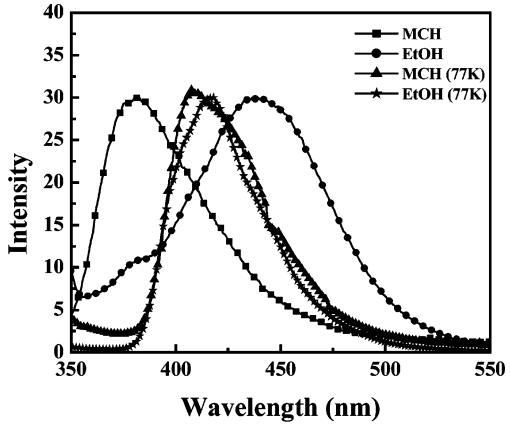

Figure 4. Emission spectra of MAPAME in methylcyclohexane (MCH) and ethanol (EtOH) at room temperature and 77 K.

pair of nitrogen, and hence, the lone pair is no longer available for the excited state charge transfer process. This establishes the fact that charge transfer occurs from the nitrogen lone pair of the monomethylamino group to the acceptor site.

We have tried to interpret this excited state phenomenon qualitatively by theoretical calculation using density functional theory. Ground state optimization for the global minimum structure of MAPAME has been done using B3LYP hybrid functional and 6-311++G(d,p) basis set. In the minimum energy ground state structure MAPAME has a planar geometry where the secondary amino and ester groups are in the plane of the benzene ring. Therefore, an extensive resonance delocalization is possible in the ground state. Selective optimized geometrical parameters are presented in Table 3. It has been proposed that the molecule with a secondary amino group already twisted in the ground state can only show dual fluorescence.[11] Otherwise the compound with a secondary amine cannot show any dual fluorescence even if in polar solvent. In the present case, the molecule has nontwisted configuration (planar) in ground state, but shows dual fluorescence in different solvent. The angular dependency of the ground and different excited states energies can be understood by rotational motion of both donor and acceptor groups around the benzene plane. Figure 5 shows the potential energy curves along the twist coordinate at the donor (θ_1) and acceptor (θ_2) groups both in vacuo and in acetonitrile solvent. In both cases, upon excitation from the planar ground state (S_0) to the S_1 state, a repulsive potential surface with a very small activation barrier, even if in gas phase, drives toward 90° twisted conformations. Both the rotational processes predict the formation of the stabilized twisted geometry in the excited state. However, energetic twisting of the acceptor group is found

TABLE 3: Optimized Geometrical Parameters for the Ground State of MAPAME in Vacuo at DFT (B3LYP/ 6-311++G(d,p)) Level

bond	calc value (Å)	angle/ dihedral angle	calc value (deg)
R_{C1-C2}	1.407	C9-N7-C1	124.52
R_{C2-C3}	1.388	C3-C4-C8	119.38
R_{C3-C4}	1.403	C8-C10-C11	120.46
R_{C1-N7}	1.372	O12-C11-O13	122.57
R_{N7-C9}	1.447	C11-O13-C14	115.76
R_{N7-H19}	1.005	C9-N7-C1-C2	0.00
R_{C4-C8}	1.452	C3-C4-C8-C10	−180.00
R_{C8-C10}	1.347	O12-C11-O13-C14	−0.00
$R_{C10-C11}$	1.468		
$R_{C11-O12}$	1.213		
$R_{C11-O13}$	1.361		

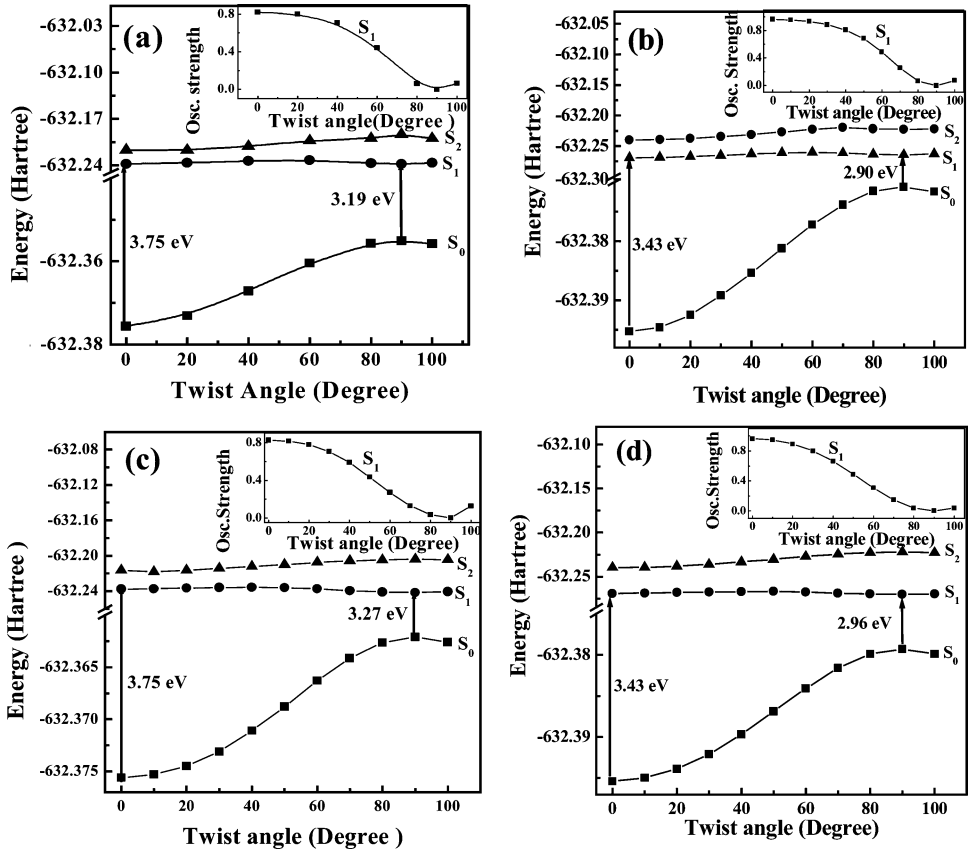

Figure 5. Potential energy surfaces for the ground and first two excited states along the twisting coordinate of the donor (−NHMe) group (a) in vacuo and (b) in acetonitrile solvent; same plot along the twisting coordinate of the acceptor (−CH═CHCOOMe) group (c) in vacuo and (d) in acetonitrile solvent using DFT (B3LYP/6-31++g(d,p)) method. Inset: plot of the variation of oscillator strength along twist coordinates.

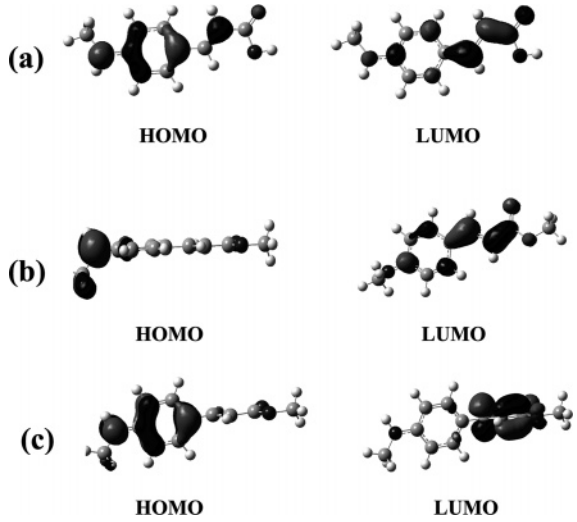

Figure 6. HOMO and LUMO molecular orbital for the (a) optimized ground state structure, twisted conformer due to the rotation of (b) donor (−NHMe) and (c) acceptor (−CH= CHCOOMe) group from same level of calculation.

TABLE 4: Comparison between the Computed Energies and Experimental Values in Vacuo and in Acetonitrile Solvent

		absorption		emission		
medium	state	E_{th}[a] (eV)	E_{ex}[b] (eV)	E_{th}[c] (eV)	E_{th}[d] (eV)	E_{ex} (eV)
vacuum	S_1	3.75	−	3.19	3.27	−
	S_2	4.32	−	4.40	4.29	−
acetonitrile	S_1	3.47	3.54	2.90	2.96	2.85
	S_2	4.26	3.89	4.03	4.27	−

[a] E_{th} is the calculated energy value ($E_{excited} - E_{ground}$) at the DFT level (B3LYP/6-311++G(d,p)). [b] E_{ex} is the experimental value. [c] Theoretical emission energy due to twisting of −NHMe group. [d] Theoretical emission energy due to twisting of the methylacrylate group.

to occurred through easier path (Figure 5c,d). An analysis of TDDFT wave functions shows that the $S_0 \rightarrow S_1$ transition for the equilibrium conformer is $\pi-\pi^*$ type, where the nitrogen lone pair is delocalized in the HOMO and the LUMO is the π^* orbital at the benzene ring site (Figure 6a). The calculated oscillator strength ($f = 0.8200$) is high as it is a $\pi-\pi^*$ transition. During the twisting of the donor group ($\theta_1 = 90°$), the CT transition is characterized by a single excitation from the HOMO nonbonding orbital to the LUMO π^* orbital (Figure 6b). In this case, the nitrogen lone pair is totally localized over the monomethylamino moiety. The calculated low oscillator strength value ($f = 0.0000$) indicates the forbidden nature of HOMO−LUMO transition (n−π^* transition). At the twisted geometry of the acceptor group ($\theta_2 = 90°$), the HOMO ($\pi_{benzene}$) is more diffused (Figure 6c). Now the single excitation is $\pi_{benzene}-\pi_{acceptor}$ type. The low calculated oscillator strength value ($f = 0.0004$) may be due to a different symmetry of the ground and excited state orbitals. In this case also the delocalization of the nitrogen lone pair in the HOMO does not support the CT process, whereas the localized nitrogen lone pair at the donor twisting geometry favors the CT process. A similar type of observation is also found in our previous works.[16,17]

Calculated absorption and emission energies are presented in Table 4. It is seen that the calculated absorption and emission energy yields good agreement with the experimental results. The deviation between the calculated and experimental transition energy in acetonitrile solvent is only 0.07 eV. The computed transition energy in acetonitrile solvent shows a red shift of ~0.28 eV relative to gas phase, indicating the polar nature of the molecule in the ground state. Calculation predicts a large Stokes shifted emission in the excited state obtained by both the twisting paths. Additionally, calculations also predict solvent dependency of the red shifted emission, and the calculated red shift of the CT band in acetonitrile solvent is about 0.29 eV.

4. Conclusion

In this paper we have presented the ICT reaction of a donor−acceptor system where the secondary amino group without ortho substitution acts as charge donor. The molecule MAPAME shows dual fluorescence in polar aprotic solvents corresponding to LE and CT emission. The high dipole moment of the excited state calculated by the solvatochromic plot supports that charge transfer occurs in the excited state. From quantum yield and lifetime values it is clear that in polar protic solvent the nature of emissive species changes due to intermolecular hydrogen bonding between the solute and solvent. Theoretically both the donor and acceptor groups are found to be planar with the benzene ring. This could be the first example where a secondary amine with nontwisted ground state geometry shows dual fluorescence. Potential energy surfaces along two twist coordinates (donor and acceptor) have been calculated at TDDFT and TDDFT-PCM levels. Theoretically both the twisting paths (both at donor side and acceptor side) favor the excited state ICT relaxation process. However, the MO picture supports that the twisting along the donor part is responsible for the excited state CT fluorescence in MAPAME molecule.

Acknowledgment. This work is supported by a grant from DST, India (Project No. SP/S1/PC-1/2003). The authors also thank Professor Tapan Ganguly, Department of Spectroscopy, IACS, and Professor Sanjib Ghosh and Mr. Subhadeep Samanta, Department of Chemistry, Presidency College, Calcutta, for allowing their low temperature and fluorescence lifetime measurements available for this work.

References and Notes

(1) Bosshard, Ch.; Sutter, K.; Pretre, P.; Hulliger, J.; Florsheimer, M.; Kaatz, P.; Gunter, P. *Organic Nonlinear Optical Materials*; Advances in Nonlinear Optics, Vol.1; Gordon and Breach: Langhorne, PA, 1995.

(2) Lakowicz, J. R. *Principles of Fluorescence Spectroscopy*, 2nd ed.; Kluwer Academic: Hongham, 1999.

(3) Kippelen, B.; Lackritz, H. S.; Claus, R. O. *Organic Nonlinear Optical Material and Devices*; P. A. Materials Research Society, 1999.

(4) Das, R.; Guha, D.; Mirta, S.; Kar, S.; Lahiri, S.; Mukherjee, S. *J. Phys. Chem. A* **1997**, *101*, 4042.

(5) Lippert, E.; Luder, W.; Moll, F.; Nagele, W.; Boos, H.; Prigge, H.; Seibold-Blankenstein, L. *Angew. Chem.* **1961**, *73*, 695.

(6) Rotkiewicz, K.; Grellmann, K. H.; Grabowski, Z. R. *Chem. Phys. Lett.* **1973**, *19*, 315.

(7) Schuddeboom, W.; Jonker, S. A.; Warman, J. M.; Leinhos, U.; Kuhnle, W.; Zachariasse, K. *J. Phys. Chem.* **1992**, *96*, 10809.

(8) Sobolewski, A. L.; Domcke, W. *Chem. Phys. Lett.* **1996**, *250*, 428.

(9) Sobolewski, A. L.; Domcke, W. *Chem. Phys. Lett.* **1996**, *259*, 119.

(10) Zachariasse, K. A.; Grobys, M.; Tauer, E. *Chem. Phys. Lett.* **1997**, *274*, 372.

(11) Grabowski, Z.; Rotkiewicz, K.; Rettig, W. *Chem. Rev.* **2003**, *103*, 3899.

(12) Rappoport, D.; Furche, F. *J. Am. Chem. Soc.* **2004**, *126*, 1277.

(13) Kohn, A.; Hattig, C. *J. Am. Chem. Soc.* **2004**, *126*, 7399.

(14) Rotkiewicz, K.; Rettig, W. *J. Lumin.* **1992**, *54*, 221.

(15) Zachariasse, K. A.; Von der Haar, T.; Hebecker, A.; Leinhos, U.; Kuhnle, W. *Pure Appl. Chem.* **1993**, *65*, 1745.

(16) Chakraborty, A.; Kar, S.; Guchhait, N. *Chem. Phys.* **2006**, *324*, 733.

(17) Chakraborty, A.; Kar, S.; Guchhait, N. *J. Photochem. Photobiol. A: Chem.* **2006**, *181*, 246.

(18) Jodicke, C. J.; Luthi, H.-P. *J. Chem. Phys.* **2002**, *117*, 4146.

(19) Jodicke, C. J.; Luthi, H.-P. *J. Chem. Phys.* **2003**, *119*, 12852.

(20) Jodicke, C. J.; Luthi, H.-P. *J. Am. Chem. Soc.* **2003**, *125*, 252.

(21) Duan, X.-H.; Li, X.-Y.; He, R.-X.; Cheng, X−M. *J. Chem. Phys.* **2005**, *122*, 84314.
(22) Cammi, R.; Mennucci, B.; Tomasi, J. *J. Phys. Chem. A* **2000**, *104*, 5631.
(23) Chowdhury, P.; Panja, S.; Chakravorti, S. *J. Phys. Chem. A* **2003**, *107*, 83.
(24) Pal, S. K.; Batabyal, S. K.; Ganguly, T. *Chem. Phys. Lett.* **2005**, *406*, 420.
(25) Bevington, P. R. *Data Reduction and Error Analysis for the Physical Sciences*; McGrawHill: New York, 1969.
(26) Frisch, M. J.; et al. *Gaussian 03*, Revision B.03; Gaussian, Inc.: Pittsburgh, PA, 2003.
(27) Casida, M. E.; Casida, K. C.; Salahub, D. R. *J. Quantum Chem.* **2002**, *70*, 933.
(28) Mennucci, B.; Cammi, R.; Tomasi, J. *J. Chem. Phys.* **1998**, *109*, 2798.
(29) Cossi, M.; Barone, V. *J. Chem. Phys.* **2001**, *115*, 4708.
(30) Cai, Z. I. ; Reimers, J. R. *J. Chem. Phys.* **2000**, *112*, 527.
(31) Gritsenko, O. V.; A. van Guibergen, S. J.; Gorling, A.; Baerends, E. J. *J. Chem. Phys.* **2000**, *113*, 8478.
(32) Neugebauer, J.; Gritsebko, O.; Jan Baerends, E. *J. Chem. Phys.* **2006**, *124*, 214102.
(33) Jamorski, C.; Foresman, J. B.; Thilgen, C.; Luthi, H.-P. *J. Chem. Phys.* **2002**, *116*, 8761.
(34) Shen, L.; Ji, H.-F.; Zhang, H.-Y. *Chem. Phys. Lett.* **2005**, *409*, 300.
(35) Jodicke, C. J.; Luthi, H.-P. *J. Chem. Phys.* **2002**, *117*, 4157.
(36) Chakraborty, A.; Kar, S.; Guchhait, N. *Chem. Phys.* **2006**, *320*, 75.
(37) Bangal, P. R.; Chakravorti, S. *J. Photochem. Photobiol. A: Chem.* **1998**, *116*, 191.
(38) Bangal, P. R.; Panja, S.; Chakravorti, S. *J. Photochem. Photobiol. A: Chem.* **2001**, *139*, 5.
(39) Mataga, N.; Kaifu, Y.; Koizumi, M. *Bull. Chem. Soc. Jpn.* **1956**, *29*, 465.
(40) Lewis, F. D.; Weigel, W. *J. Phys. Chem. A* **2000**, *104*, 8146.
(41) Taft, R. W.; Kamlet, M. J. *J. Am. Chem. Soc.* **1976**, *98*, 2886.
(42) Testa, A. C. *J. Lumin.***1991**, *50*, 243.
(43) Fischer, E. *J. Phys. Chem.* **1973**, *77*, 859.
(44) Catalan, J.; Zinanyi, L.; Saltiel, J. *J. Am. Chem. Soc.* **2000**, *122*, 2377.